

Advances in Transdisciplinary Engineering series

volume 58

Advances in Machinery, Materials Science and Engineering Application X



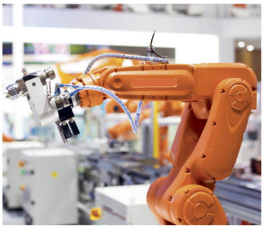

Proceedings of the 10th International Conference (MMSE 2024), Paris, France, 27-28 July 2024

EDITED BY
Marco Giorgetti
Ramesh K. Agarwal
Min Chen
Hao Peng

IOS Press

Advances in Machinery, Materials Science and Engineering Application X
M. Giorgetti et al. (Eds.)

doi:10.3233/ATDE240666

Nonlinear Vibration Isolator with Softening Spring and Nonlinear Damping

Volodymyr PUZYROV [a,b], Nataliya LOSYEVA [a,b] and Nina SAVCHENKO [c,1]
[a] *Universidad de Barcelona, Spain*
[b] *Nizhyn Mykola Gogol State University, Ukraine*
[c] *National Aerospace University KhAI, Ukraine*

Abstract. In recent decades, nonlinear isolators have become widely used to solve problems of passive isolation of unwanted vibrations. A special place is occupied by nonlinear stiffness isolation supports, which provide high static stiffness along with low dynamic stiffness or even quasi-zero stiffness (QZS) in the displacement range. These vibration isolators provide a higher isolation bandwidth with low transfer capacity than conventional linear devices. In this paper, nonlinear single-degree of freedom (DOF) vibration isolator with quadratic and cubic nonlinear stiffness components and a quadratic damping component is analyzed. The system responses and magnitude of force transmissibility in the vicinity of resonant frequency are analyzed. The dynamic response is obtained using the harmonic balance method. A significant contribution from the quadratic component of the damping force is emphasized. Also asymptotical formulas for responses magnitude, resonant frequency and force transmissibility there are presented, which allow optimizing the choice of the parameters of the isolator more easily.

Keywords. Nonlinear vibration isolator, nonlinear damping, harmonic balance method, force transmissibility

1. Introduction

The use of passive type isolators is one of the widely used methods to control unwanted vibrations [1]. The characteristics of passive linear isolators have been widely studied [2, 3]. The simplest case of linear passive isolation is that a mass m is supported by a linear spring k on a rigid base, and vibration isolation can be achieved in the region of excitation frequency $\Omega > \sqrt{2}\Omega_0$, where Ω_0 is the natural frequency of the linear isolation system. The isolation efficiency of a linear isolator is limited by frequency range. In order to improve the efficiency, nonlinear isolators with high static and low dynamic stiffness have been proposed [4]. High static stiffness implies small deflection and large load, and low dynamic stiffness implies a wide range of isolation frequencies. The stiffness of nonlinear isolators can be realized by combining positive stiffness with negative stiffness to form a near-zero stiffness at the operating point, which is referred to in the literature as quasi-zero stiffness (QZS) characteristics [5, 6].

[1] Nina SAVCHENKO, Corresponding author, National Aerospace University KhAI, Ukraine; E-mail: n.savchenko@khai.edu.

Numerous types of designs have been proposed by various authors such as coil spring structures [7], plate or rod spring structures [8], cam-roller structures [9], and many others.

The idea of using the inclined springs to achieve quasi-zero stiffness of the isolator was discussed in the paper [10]. Zheng et al. [11], proposed a negative stiffness magnetic spring (NSMS). The NSMS, consisting of a pair of coaxial ring permanent magnets, was installed parallel to the mechanical spring to counteract its positive stiffness. Also in the work of [12], a nonlinear absorber with a negative stiffness magnetic spring was proposed. Various aspects of mitigation of the responses of the isolated structure were discussed in papers [13 – 15].

In this study we continue the analysis of the behavior of such a dynamic system, partially presented in the paper [16]. We show a significant influence of the quadratic component of damping on the magnitude of the responses of the structure and the force transmissibility. An analytical procedure for approximately finding the magnitude of responses is also proposed.

2. Formulation of the Problem

Consider the following equation

$$m\ddot{x} + c_1\dot{x} + c_2\,\dot{x}\,|\dot{x}| + f(x) = m\,A\,\omega^2 \cos(\omega\, t), \tag{1}$$

where $f(x) = k_{lin}\,x + k_2\,x^2 + k_3\,x^3$,which describes the motion of a mass under the action of a nonlinear restoring force, nonlinear friction force and external harmonic excitation (figure 1).

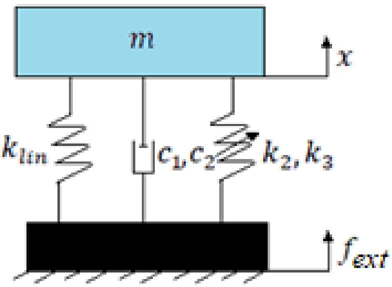

Figure 1. Schematic view of nonlinear vibration isolator.

Let us introduce the dimensionless variables and parameters according formulas

$$x = A\,\tilde{x}, c_1 = m\,\omega_1\,\zeta_1, k_{lin} = \kappa_1 m\,\omega_1^2, k_2 = \kappa_1\kappa_2/A, k_3 = \kappa_1\kappa_3/A^2,$$

$$\omega_1 t = \tau,\ \omega/\omega_1 = \Omega. \tag{2}$$

In fact, below we assume that $k_{lin} = m\,\omega_1^2$ $(\kappa_1 = 1)$, but in the case when k_{lin} is small (the case of quasi-zero stiffness), preserving the parameter κ_1 in the subsequent formulas is useful.

We rewrite equation (1) in the form

$$\tilde{x}'' + \zeta_1\, \tilde{x}' + \zeta_2 \tilde{x}' |\tilde{x}'| + \kappa_1\, \tilde{x} + \kappa_2\, \tilde{x}^2 + \kappa_3 \tilde{x}^3 = \Omega^2 \cos(\Omega\, \tau). \tag{3}$$

Based on Harmonic Balance (HB) method we seek the solution of equation (3) in the following form

$$x(\tau) = X_0 + X_1 \cos(\Omega\, \tau + \phi). \tag{4}$$

Substituting expression (4) into equation (3), taking into account that

$$\cos(\Omega\, \tau) = \cos(\Omega\, \tau + \phi - \phi) = \cos\phi \cos(\Omega\, \tau + \phi) + \sin\phi \sin(\Omega\, \tau + \phi)$$

and limiting ourselves to first-order harmonics, we have

$$\Phi_1 = 2\, \kappa_1\, X_0 + \kappa_2\, (X_1^2 + 2\, X_0^2) + \kappa_3\, X_0\, (3\, X_1^2 + 2\, X_0^2) = 0, \tag{5}$$

$$X_1 \left[-\Omega^2 + \kappa_1 + 2\, X_0\, \kappa_2 + 3\, \kappa_3 \left(X_0^2 + \tfrac{1}{4}\, X_1^2 \right) \right] = \Omega^2 \cos\phi\,, \tag{6}$$

$$-\Omega\, X_1 \left(\zeta_1 + \tfrac{8}{3\pi}\, \Omega\, \zeta_2\, X_1\, sgn\, X_1 \right) = \Omega^2 \sin\phi. \tag{7}$$

Assuming $X_1 > 0$, from equalities (6), (7) we conclude

$$\Phi_2\, (X_0, X_1, \Omega, \zeta_1, \zeta_2, \kappa_1, \kappa_2, \kappa_3) = 0 \tag{8}$$

where

$$\Phi_2 = \tfrac{9}{16}\, \kappa_3^2\, X_1^6 + \tfrac{1}{2} \left[\tfrac{128}{9\pi^2}\, \zeta_2^2\, \Omega^4 - 3\, \kappa_3\, \Omega^2 + 3\, \kappa_3\, (3\, \kappa_3\, X_0^2 + 2\, \kappa_2\, X_0 + \kappa_1) \right] X_1^4 + \tfrac{16}{3\pi}\, \zeta_1\, \zeta_2\, \Omega^3\, X_1^3 + \{ \Omega^4 - (6\, \kappa_3\, X_0^2 + 4\, \kappa_2\, X_0 + 2\, \kappa_1 - \zeta_1^2) \Omega^2 + [(3\, \kappa_3\, X_0 + \kappa_2)^2 + 3\, \kappa_1\, \kappa_2 - \kappa_2^2]\} X_1^2 - \Omega^4, \tag{8a}$$

3. Parametric Analysis of the Frequency-Amplitude Relation

In this section we want to evaluate the influence of the mechanical parameters of the isolator on the value of $x(\Omega)$. Since we cannot write X_0, X_1 as an explicit functions of these parameters, we will express X_1 from equality (5)

$$\tilde{X}_1(X_0) = \sqrt{\frac{2\, X_0 (\kappa_1 + \kappa_2\, X_0 + \kappa_3\, X_0^2)}{-\kappa_2 - 3\, \kappa_3 X_0}} \tag{9}$$

Substituting the found expression into equality (8), we obtain $\tilde{\Phi}_2\, (X_0) = 0$, where the expression $\tilde{\Phi}_2\, (X_0)$ is quite cumbersome, but has an algebraic structure and can be used to analyze the influence of parameters on the value of $\max \tilde{x}(\tau)$.

Provided that the parameters of the isolator are given, the equality (8) defines the value of X_0 as an implicit function of the argument Ω. Thus, the maximum value of the oscillation amplitude is achieved at the frequency value corresponding to the condition

$$\left(\frac{d\tilde{X}_1}{dX_0} + 1\right)\frac{\partial X_0}{\partial \Omega} = 0. \tag{10}$$

Remark. For the variety of values of parameters $\kappa_1, \kappa_2, \kappa_3$ the first multiplier in left-hand side of (10) takes non-zero values – the solutions with respect to X_0 are complex.

Differentiating the implicit function $\Phi_2\ (X_1, X_0, \Omega)$ we have

$$\frac{d\tilde{\Phi}_2(\Omega)}{d\Omega} = \frac{\partial\tilde{\Phi}_2}{\partial X_0}\frac{\partial X_0}{\partial \Omega} + \frac{\partial\tilde{\Phi}_2}{\partial \Omega} = \frac{\partial\tilde{\Phi}_2}{\partial \Omega} = 0. \tag{11}$$

Taking into account the presence of a nonlinear damping component, the frequency-amplitude relation (8a) contains a cubic term relative to Ω. This does not allow, in contrast to many works (for example, [5, 17]), to write down the resonant frequencies in an explicit (relatively compact) form. For given values of the damping and stiffness parameters, a resonant frequency values may be presented in graphical form on a plane $X_0\Omega$ as a line of intersection of surfaces

$$\Phi_2\ (X_1\ (X_0), X_0, \Omega) = 0, \quad \frac{\partial\Phi_2}{\partial\Omega} = 0. \tag{12}$$

The frequency-amplitude curve as intersection of surfaces $\Phi_2\ (X_0, \Omega)$ and $X = X_0 + \tilde{X}_1\ (X_0)$ is presented in figure 2.

Also in the next section a method for approximately finding these frequencies will be described.

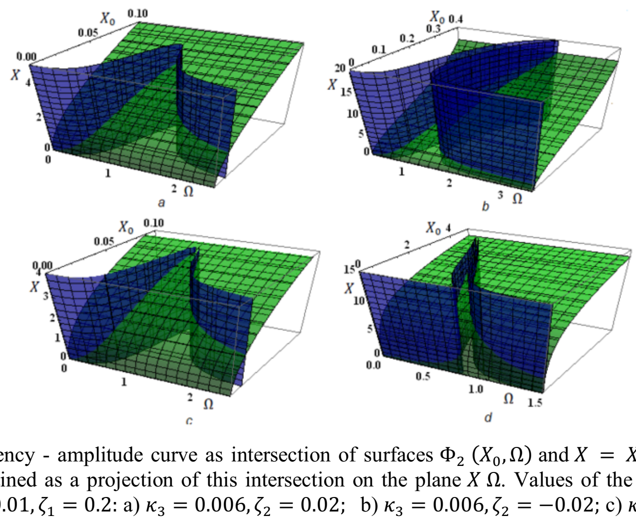

Figure 2. Frequency - amplitude curve as intersection of surfaces $\Phi_2\ (X_0, \Omega)$ and $X = X_0 + \tilde{X}_1\ (X_0)$. The 2D curve is obtained as a projection of this intersection on the plane $X\ \Omega$. Values of the parameters are κ_1 $\kappa_1 = 1, \kappa_2 = -0.01, \zeta_1 = 0.2$: a) $\kappa_3 = 0.006, \zeta_2 = 0.02$; b) $\kappa_3 = 0.006, \zeta_2 = -0.02$; c) $\kappa_3 = -0.006, \zeta_2 = 0.02$; d) $\kappa_3 = -0.006, \zeta_2 = -0.02$.

Remark. The system of equations (12) although being an algebraic, has very high order, and finding its solution by numerical methods is not very effective (it is computation costly and allowing for a large error). Therefore, it is more advantageous to find a pair of values (X_0, Ω_{res}) graphically, as shown in figure 3.

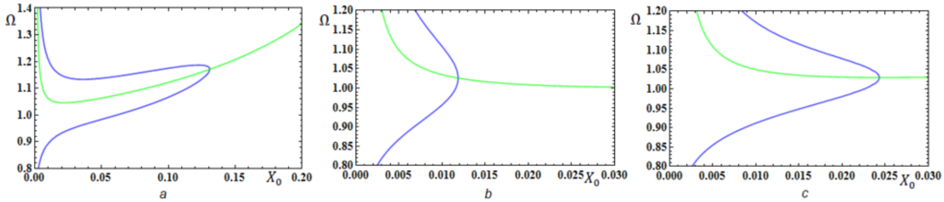

Figure 3. Graphical determination of resonant frequency for different values of quadratic damping component. $\kappa_1 = 1, \kappa_2 = -0.002, \kappa_3 = 0.002$: a) $\zeta_2 = -0.03$; b) $\zeta_2 = 0.03$; c) $\zeta_2 = 0$.

Some results of numerical calculations are presented in the table 1.

Table 1. Magnitudes of X_0, Ω_{res}, X_1 calculated for different values of nonlinear parameters of the isolator ($\zeta_1 = 0.2$).

ζ_2	κ_2	κ_3	X_0	Ω	X_1
-0.03	-0.002	-0.004	0.136	0.895	8.652
0.03	-0.002	-0.004	0.0127	0.997	3.435
0	-0.002	-0.004	0.0271	0.974	4.828
0	-0.002	-0.004	-0.0271	0.975	4.828
0	-0.002	0.004	-0.0237	1.049	5.25
0	-0.002	0.004	0.231	1.05	5.256
-0.01	0.004	-0.001	-0.101	0.974	6.62
0.01	0.004	-0.001	-0.0376	0.999	10.954

As can be seen from table 1, the positive quadratic component of damping significantly reduces the magnitude of the peak responses.

4. Asymptotic Representation of the Resonant Frequency and Magnitude of System Responses

Note, that the problem of determining the optimal set of isolator parameters for an arbitrary set of the values $\zeta_1, \zeta_2, \kappa_2, \kappa_3$ may be very labor-intensive, because equalities (5), (8) contain seven unknown variables.

Therefore, to reduce the computational procedures, one can use previously the asymptotic representation of these values. Indeed, for a specific mechanical system, due to the existing technical limitations, the orders of magnitude are usually predetermined. As a rule, the dimensionless parameters are small, while the last three have an order of smallness higher than Ω.

Considering that Ω is of the order of unity, and, in addition, we want to estimate the influence of the nonlinear component of stiffness, then the term $\kappa_3^2 X_1^6$ should also have a zero order of smallness. Accordingly, introducing a small parameter in an artificial way, we can write

$$\zeta_1 = \varepsilon\,\tilde{\zeta}_1, \zeta_2 = \varepsilon^3\,\tilde{\zeta}_2,\ \kappa_2 = \varepsilon^3\,\tilde{\kappa}_2,\ \kappa_3 = \varepsilon^3\,\tilde{\kappa}_3, (\kappa_1 = 1)$$

$$X_0 = \varepsilon\,(X_{00} + \varepsilon\, X_{01}), \quad X_1 = \frac{1}{\varepsilon}\,(X_{10} + \varepsilon\, X_{11}), \Omega = 1 + \varepsilon\,\Omega_1.$$

The first iteration results on $X_{00} = 0,\ \Omega_0 = 1.$

The second iteration leads to algebraic system

$$2\,\mathrm{X}_{01} + \tilde{\kappa}_2\,\mathrm{X}_{10}^2 = 0,$$

$$9\,\mathrm{X}_{10}^6\,\tilde{\kappa}_3^2 - 48\,\mathrm{X}_{10}^4\,\tilde{\kappa}_3\,\Omega_1 + 16\,(\tilde{\zeta}_1^2 + 4\,\Omega_1^2) - 16 = 0,$$

$$\mathrm{X}_{10}^2\,(3\,\mathrm{X}_{10}^2\,\tilde{\kappa}_3 - 8\,\Omega_1) = 0.$$

Expressing Ω_1 from the third equation we find in series

$$X_{10} = \frac{1}{\tilde{\zeta}_1}, X_{01} = -\frac{\tilde{\kappa}_2}{2\tilde{\zeta}_1^2}, \Omega_1 = \frac{3\,\tilde{\kappa}_3}{8\,\tilde{\zeta}_1^2}.$$

The third iteration leads to

$$X_{11} = \frac{1}{24\tilde{\zeta}_1^3}\left(9\,\tilde{\kappa}_3 - \frac{64}{\pi}\,\tilde{\zeta}_2\right), \Omega_2 = \frac{1}{128\tilde{\zeta}_1}\left(27\,\tilde{\kappa}_3^2 + 32\,\tilde{\zeta}_1^6 - \frac{256}{\pi}\,\tilde{\kappa}_3\,\tilde{\zeta}_2\right),$$

$$X_{02} = \frac{1}{24\tilde{\zeta}_1^3}\left(9\,\tilde{\kappa}_3 - \frac{64}{\pi}\,\tilde{\zeta}_2\right), etc.$$

Consequently, we have

$$X_0 \approx -\frac{\kappa_2}{2\zeta_1^2} + \frac{\kappa_2}{24\zeta_1^4}\left(\frac{64}{\pi}\zeta_2 + 9\kappa_3\right), \quad X_1 \approx \frac{1}{\zeta_1} - \frac{1}{24\zeta_1^3}\left(\frac{64}{\pi}\,\zeta_2 - 9\kappa_3\right), \tag{13}$$

$$\Omega_{res} \approx 1 + \frac{3\kappa_3}{8\zeta_1^3} + \frac{1}{128\zeta_1^4}\,(27\kappa_3^2 - \frac{256}{\pi}\,\zeta_2\,\kappa_3 + 32\,\zeta_1^6).$$

Although the formulas (13) are approximate, they give a pretty good estimation of magnitude (dimensionless) of system responses. In particular, for the first three rows from table 1 we have $9.39, 3.50, 4.99$ vs $8.65, 3.44, 4.83$ respectively.

The non-dimensional force transmitted through the nonlinear coupling that comprises the isolator, presented in figure 1, is defined as

$$F_{tr} = \zeta_1\,\tilde{x}' + \zeta_2\,\tilde{x}'\,|\tilde{x}'| + \tilde{x} + \kappa_2\,\tilde{x}^2 + \kappa_3\,\tilde{x}^3.$$

Applying again HB method we can present the first-order harmonic of the transmitted force in the form $F_{tr} = F\cos(\Omega\,\tau + \phi_1)$, and the magnitude of the force is given by

$$F = \sqrt{X_1^2\,\left[\kappa_1 + 2\kappa_2\,X_0 + 3\,\kappa_3\,\left(X_0^2 + \frac{1}{4}\,X_1^2\right)\right]^2 + \Omega^2\,X_1^2\,\left(\zeta_1 + \frac{8}{3\pi}\,\zeta_2\,\Omega\,X_1\right)^2}. \tag{14}$$

Thus, the dimensionless force transmissibility is

$$T_F = \frac{F}{\Omega^2}. \tag{15}$$

In order to examine the influence of the parameters of isolator on magnitude of T_F we can use the same methodology as in previous section, e.g. consider the intersection of hyper-surfaces (8) and (15).

Also, substituting formulas (13) into expression (15), we obtain an approximate formula

$$T_F \approx \frac{1}{\zeta_1}\sqrt{1 + \frac{1}{12\zeta_1^2}\left(9\,\kappa_3 - \frac{64}{\pi}\,\zeta_2\right)}. \tag{16}$$

The force transmissibility curve according to formula (16) is presented in figure 4.

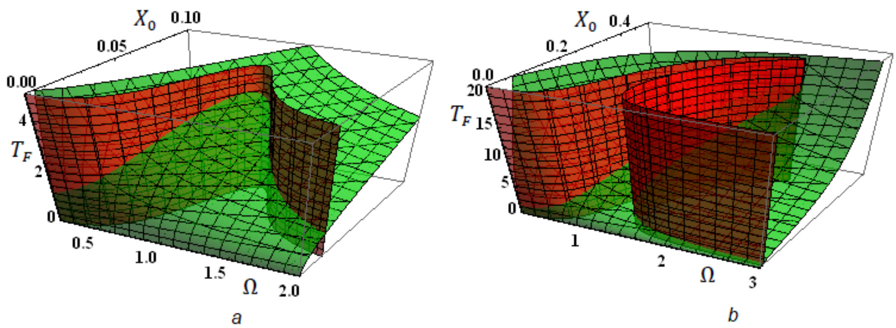

Figure 4. Force transmissibility curve according to formula (16). Values of the parameters are $\kappa_1 = 1, \kappa_2 = -0.01, \zeta_1 = 0.2$: a) $\kappa_3 = 0.006, \zeta_2 = 0.02$; b) $\kappa_3 = 0.006, \zeta_2 = -0.02$;

As one can see in figure 5, the magnitude of responses increases drastically for hardening spring (50 times or more) – the far right side corresponds to positive values of κ_2, κ_3.

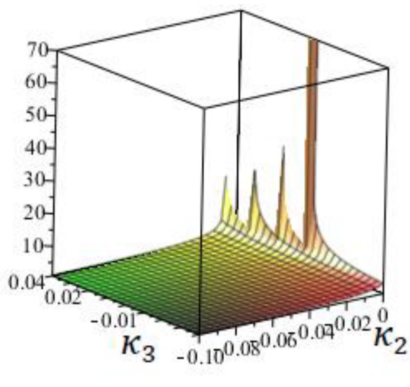

Figure 5. Dependence of magnitude of X_1 on nonlinear stiffness components.

5. Conclusion

A single-DOF nonlinear dynamical system which describes the vibration isolator is studied. The nonlinear components consist of quadratic damping force and quadratic and cubic stiffness terms. The system responses and magnitude of force transmissibility in the vicinity of resonant frequency are analyzed. Besides the qualitative features (softening spring is much more efficient then hardening one and "hardening" damping is welcomed), the approximate formulas are presented, which allow optimizing the choice of the parameters of the isolator more easily. Analytical conclusions are supported by numerical simulations.

The future work involves developing an analytical algorithm for optimizing nonlinear characteristics of the isolator and applying this approach to several types of devices described in the literature.

Author Contributions

Conceptualization, Puzyrov V; Data curation, Puzyrov V and Losyeva N; Formal analysis, Puzyrov V; Methodology, Puzyrov V; Software, Puzyrov V and Savchenko N; Supervision, Puzyrov V and Losyeva N; Validation, Puzyrov V and Savchenko N; Visualization, Puzyrov V and Savchenko N; Writing –original draft, Puzyrov V; Writing – review & editing, Puzyrov V, Losyeva N and Savchenko N. All authors have read and agreed to the published version of the manuscript.

References

[1] Harris CM, Piersol AG. Shock and Vibration Handbook. McGraw-Hill, New York, 2002.
[2] Crede CE. Vibration and Shock Isolation. Wiley, New York, 1995.
[3] Den Hartog JP. Mechanical Vibrations. McGraw-Hill, New York, 1962
[4] Ibrahim RA. Recent advances in nonlinear passive vibration isolators. Journal of Sound and Vibration. 2008; 314: 371–452.
[5] Carrella A, Brennan MJ, Kovacic I, Waters TP. On the force transmissibility of a vibration isolator with quasi-zero-stiffness. Journal of Sound and Vibration. 2009; 322: 707–717.
[6] Shaw AD, Neild SA, Wagg DJ. Dynamic analysis of high static low dynamic stiffness vibration isolation mounts. Journal of Sound and Vibration. 2013; 332: 1437–1455.
[7] Le TD, Ahn KK. Experimental investigation of a vibration isolation system using negative stiffness structure. Int. J. Mech. Sci. 2013; 70: 99–112.
[8] Liu XT, Huang XC, Hua HX. On the characteristics of a quasi-zero stiffness isolator using Euler buckled beam as negative stiffness corrector. J. Sound Vib. 2013; 332: 3359–3376.
[9] Zhou JX, Wang XL, Xu DL, Bishop S. Nonlinear dynamic characteristics of a quasi-zero stiffness vibration isolator with cam–roller–spring mechanisms. J. Sound Vib. 2015; 346: 53–69.
[10] Zhao F, Ji JC, Ye K, Luo Q. Increase of quasi-zero stiffness region using two pairs of oblique springs, Mechanical Systems and Signal Processing. 2020; 144: 106975.
[11] Zheng Y, Zhang X, Luo Y, Yan B. Design and experiment of a high-static-low-dynamic stiffness magnetic spring. Journal of Sound and Vibration. 2016; 360: 31-52.
[12] Dong G, Li Q, Zhang X. Vibration attenuation using a nonlinear dynamic vibration absorber with negative stiffness. Int. J. Appl. Electromagn. Mech. 2019; 59(2): 617–28.

[13] Puzyrov V, Losyeva N, Savchenko N. On mitigation of oscillations of a mechanical system with two degrees of freedom in the vicinity of external resonances. Journal of Theoretical and Applied Mechanics. 2023; 61(3): 613-624.
[14] Gatti G, Shaw AD, Gonçalves PJP, Brennan MJ. On the detailed design of a quasi-zero stiffness device to assist in the realisation of a translational Lanchester damper. Mechanical Systems and Signal Processing. 2022; 164: 108258
[15] Yang J, Jiang JZ, Neild SA. Dynamic analysis and performance evaluation of nonlinear inerter-based vibration isolators. Nonlinear Dyn. 2020; 99: 1823–1839.
[16] Wang K, Zhou JX, Chang YP, Ouyang HJ, Xu D, Yang Y. A nonlinear ultra-low-frequency vibration isolator with dual quasi-zero-stiffness mechanism. Nonlinear Dyn. 2020; 101(2): 755–773.
[17] Puzyrov V, Losyeva N, Savchenko N. Parametric analysis of the dynamics of a nonlinear vibration isolator. Advances in Transdisciplinary Engineering. 2023: 391-396. doi: 10.3233/ATDE230485